

7-10 May 2024 - Consiglio Nazionale delle Ricerche, Rome, Italy  
Standard Model at the LHC 2024

# Heavy Flavour production and spectroscopy at the LHC

---

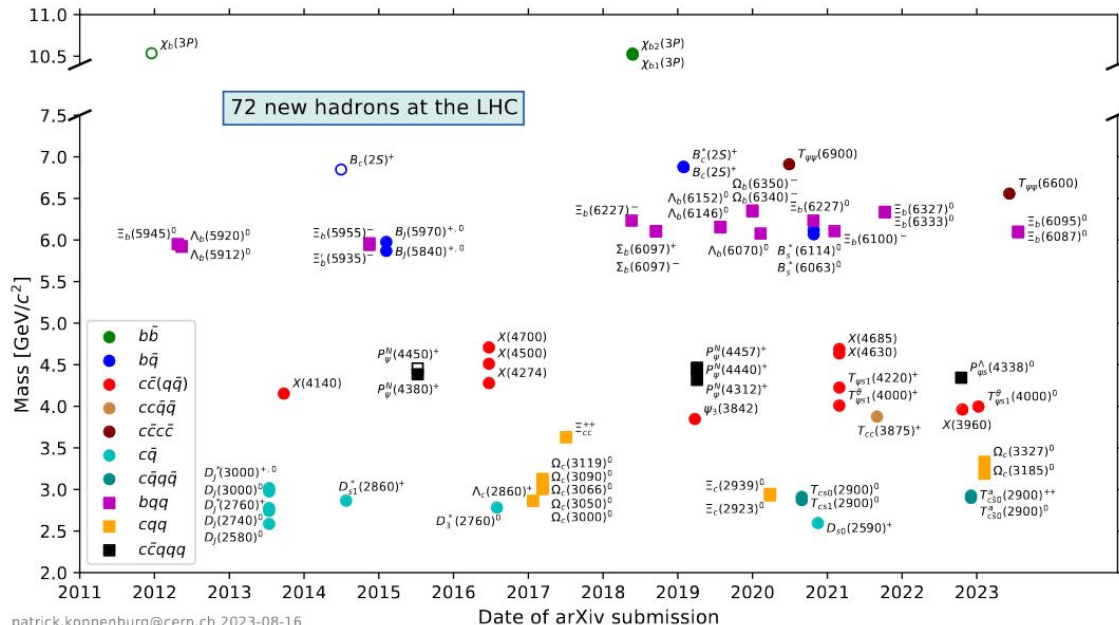
Speaker:  
Vincenzo Mastrapasqua  
on behalf of the ATLAS, CMS and LHCb Collaborations

# Heavy Flavour Physics at the LHC

LHC provides high luminosity for heavy flavour physics processes

Heavy flavor production cross section several order of magnitudes greater than at e-e colliders,

but the hadron collisions environment is characterized by **complex initial state and high background**



72 new hadrons discovered at LHC since its start!  
23 new exotics hadrons

[LHCb-FIGURE-2021-001, 2024 updated](#)

- **Structures in the di-charmonium mass spectrum**

- **LHCb:** [Sci. Bull. 65 \(2020\) 23](#)
- **CMS:** [PRL 132 \(2024\) 111901](#)
- **ATLAS:** [PRL 131 \(2023\) 151902](#)

- **Charmonium production:**

- **ATLAS:** Measurement of the production cross section of  $J/\psi$  and  $\psi(2S)$  [[EPJC 84 \(2024\) 169](#)]
- not discussed ○ **LHCb:** Measurement of associated  $J/\psi$ - $\psi(2S)$  production cross section [[arXiv](#), submitted to JHEP]
- not discussed ○ **LHCb:**  $J/\psi$ -pair production and gluon transverse-momentum dependent PDFs [[JHEP 03 \(2024\) 088](#)]

- **Conventional spectroscopy:**

- **CMS:** Observation of  $\Xi_b^- \rightarrow \psi(2S)\Xi^-$  and studies of  $\Xi_b^{*0}$  [[arXiv](#), submitted to PRD]
- **LHCb:** Observation of new baryons in  $\Xi_b^- \pi^+ \pi^-$  and  $\Xi_b^0 \pi^+ \pi^-$  systems [[PRL 131 \(2023\) 171901](#)]

- **Exotic spectroscopy:**

- **LHCb:** First observation of the  $\Lambda_b^0 \rightarrow D^+ D^- \Lambda$  decay [[arXiv](#), submitted to JHEP]
- **LHCb:** Search for prompt production of pentaquarks [[arXiv](#), submitted to PRD]
- not discussed ○ **LHCb:** First observation of  $\Lambda_b^0 \rightarrow \Sigma_c^{(*)++} D^{(*)-} K^-$  [[arXiv](#), submitted to PRD Lett]
- **CMS:** Observation of  $\Lambda_b^0 \rightarrow J/\psi \Xi^- K^+$  [[arXiv](#), submitted to EPJC]

# X(6900) at LHCb in 2020

$J/\psi J/\psi$  ( $\rightarrow 4\mu$ ) spectrum studied at LHCb using  $9 \text{ fb}^{-1}$  of pp collisions at  $\sqrt{s} = 7, 8, 13 \text{ TeV}$

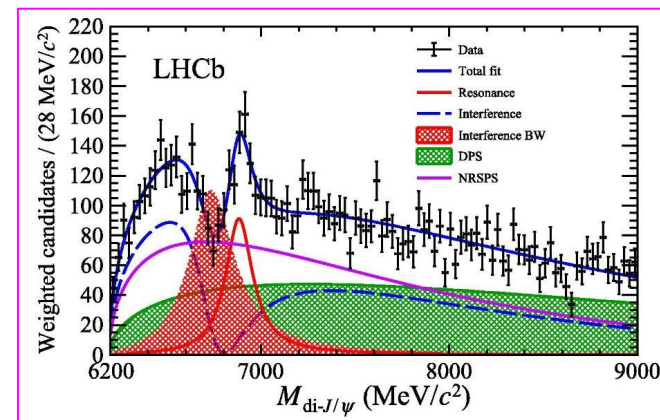
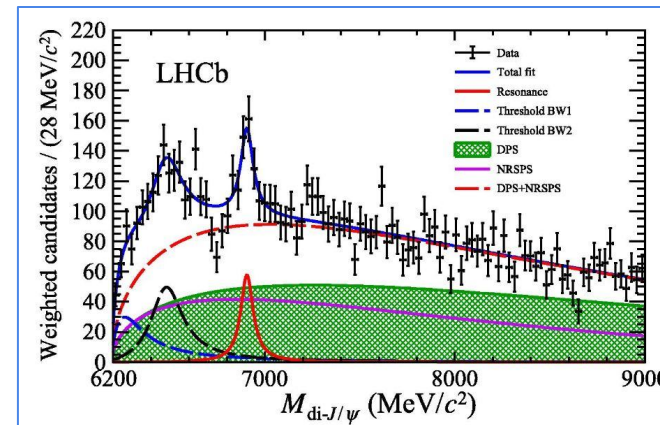
Background contribution for  $J/\psi$ -pair production:

- NRSPS (Non-Resonant Single Parton Scattering)
- DPS (Double Parton Scattering)

Two different signal models are considered:

- (top) poor description of the “dip” at 6.7 GeV
  - background DPS + NRSPS
  - relativistic Breit-Wigner for X(6900)
  - two auxiliary BWs near kinematic threshold
- (bottom)
  - background DPS + NRSPS
  - relativistic Breit-Wigner for X(6900)
  - a BW (X(6700)) to interfere with NRSPS

A broad structure near the di- $J/\psi$  mass threshold and a narrow resonance, X(6900), renamed  $T_{\psi\psi}(6900)$  reported

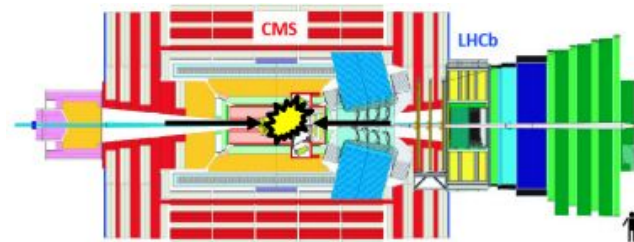


# X(6900) at CMS: background description

$J/\psi J/\psi$  ( $\rightarrow 4\mu$ ) studied at CMS using  $135 \text{ fb}^{-1}$  of pp collisions at  $\sqrt{s} = 13 \text{ TeV}$  (2016-2018)

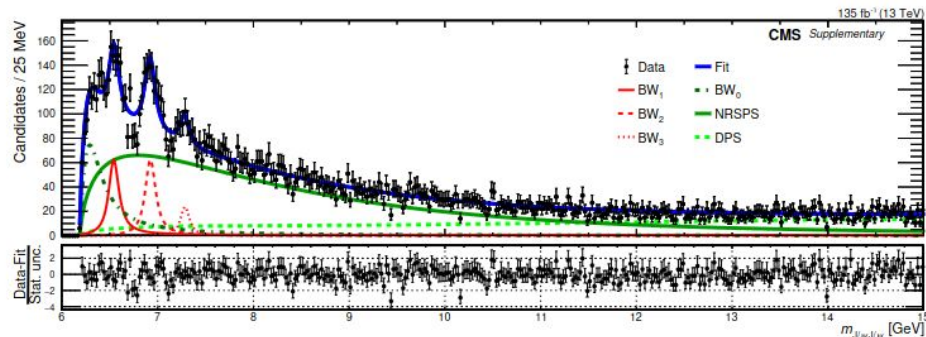
**Different background modelling** (different acceptance):

- **NRSPS** and **DPS**: parameterizations from MC
- **BW<sub>0</sub>** near  $J/\psi J/\psi$  threshold takes into account for
  - inadequacy of NRSPS near threshold
  - feed-down of partially reconstructed higher mass states
  - possible coupled-channel interactions, pomeron-exchange processes, etc.
- **Signal model**: three BWs with Gaussian resolution from MC (ranging from 10 MeV @ 6.5 GeV to 18 MeV @ 7.3 GeV)



Fit on full spectrum up to 15 GeV to verify the adequacy of the background model:  $P(\chi^2) = 98\%$

Fit fractions: 58% NRSPS, 25% DPS, 9% BW<sub>0</sub>

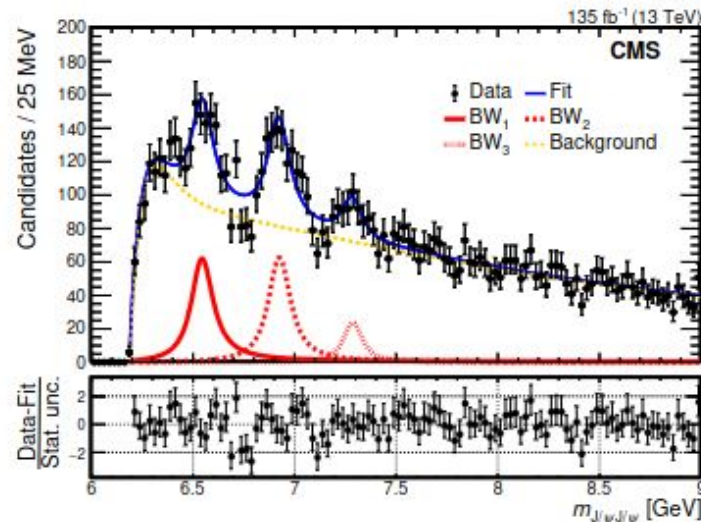


# X(6900) at CMS: non-interfering resonances

Fit features are added by checking sequentially their local statistical significance ( $> 3\sigma$  required)

signal model: **3 non-interfering scalar Relativistic BW**

Result: **poor description of dips at 6750 MeV and 7150 MeV** and overall poor fit  $P(\chi^2) = 9\%$  in the signal region



The description is improved by including interference between the three BW states (see next slide)

The two LHCb models - with NRSPS interfering with BWs - are also investigated (see backup): no improvement on fit.

NRSPS interfering with BWs is considered less probable as it is a mixture of  $J^{PC}$  states

	Mass (MeV)	Width (MeV)	Local stat. signif.
<b>BW<sub>1</sub></b>	$6552 \pm 10 \pm 12$	$124^{+32}_{-26} \pm 33$	$6.5\sigma$
<b>BW<sub>2</sub></b>	$6927 \pm 9 \pm 4$	$122^{+24}_{-21} \pm 18$	$9.4\sigma$
<b>BW<sub>3</sub></b>	$7287^{+20}_{-18} \pm 5$	$95^{+59}_{-40} \pm 19$	$4.1\sigma$

first error is statistic, second is systematic

**X(6900) confirmed at CMS. Values consistent with LHCb.**

# X(6900) at CMS: interfering resonances

**Signal model with interference:** improved fit  $P(\chi^2) = 65\%$

“three-way” interference term (three  $J^P = 0^+$  resonances)

$$|r_1 \exp(i\phi_1) BW_1 + r_2 BW_2 + r_3 \exp(i\phi_3) BW_3|^2$$

Local statistical significance improved for each signal  
(least significant:  $BW_3$   $4.7\sigma$ )

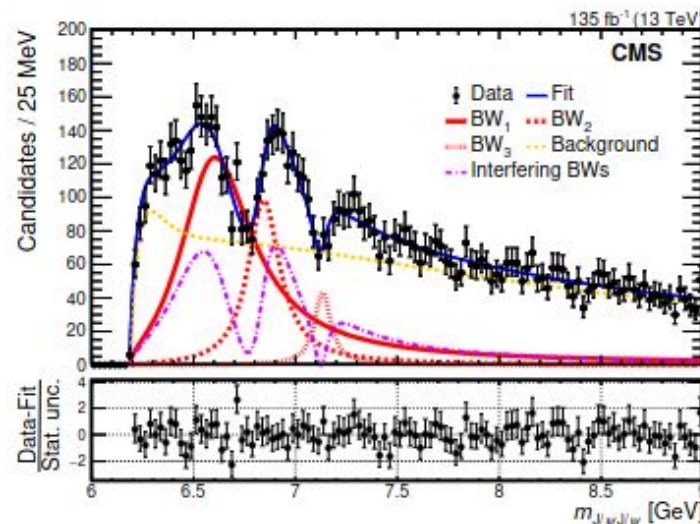
Global significance for  $BW_3$  with MC pseudo-experiments:  $3.4\sigma$

**Better fit w.r.t. any “two-way” interference option** ( $P(\chi^2) < 30\%$ )

**Improved descriptions of the dips**

**Two structures** (X(6600) and X(7100)) **appear with X(6900)**

**X(6900) is compatible with the LHCb observation** within  $2\sigma$



	Mass (MeV)	Width (MeV)
$BW_1$	$6638^{+43}_{-38} \quad ^{+16}_{-31}$	$440^{+230}_{-200} \quad ^{+110}_{-240}$
$BW_2$	$6847^{+44}_{-28} \quad ^{+48}_{-20}$	$191^{+66}_{-49} \quad ^{+25}_{-17}$
$BW_3$	$7134^{+48}_{-25} \quad ^{+41}_{-15}$	$97^{+40}_{-29} \quad ^{+29}_{-26}$

first error is statistic, second is systematic error

# X(6900) at ATLAS

$J/\psi J/\psi$  and  $J/\psi + \psi(2S)$  in  $4\mu$  final state studied at ATLAS using  $140 \text{ fb}^{-1}$  of pp collisions at  $\sqrt{s} = 13 \text{ TeV}$

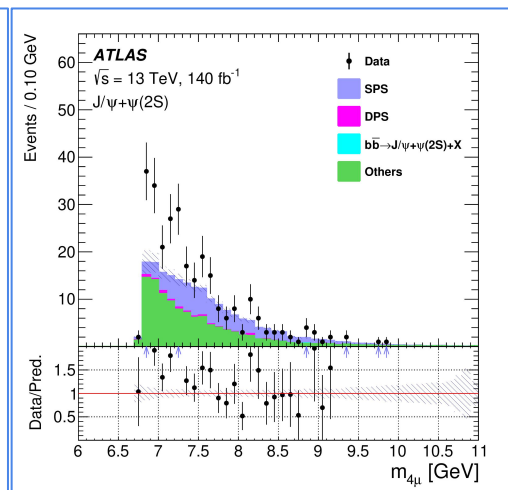
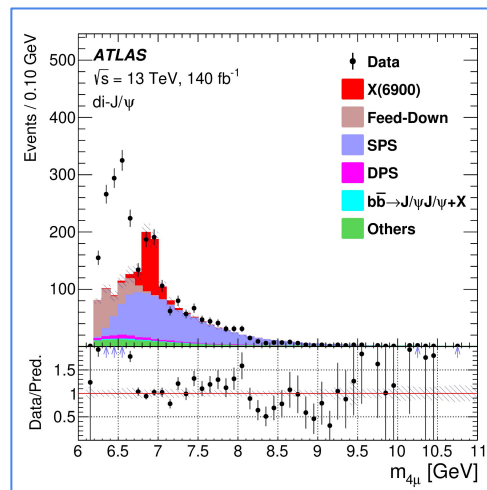
Prompt (SPS, DPS) and non-prompt ( $b\bar{b} \rightarrow J/\psi J/\psi + X$ ) background contributions are considered

Feed-down included only for di- $J/\psi$  channel

## $4\mu$ mass data vs background predictions before fit for $J/\psi J/\psi$ and $J/\psi + \psi(2S)$

**Signal model: interfering BWs  $\otimes$  Gaussian resolution** (introduced gradually to improve the fit)

- $J/\psi J/\psi$  signal:
  - A) 3 interfering scalar BWs
  - B) 2 interfering scalar BWs, the first interferes also with SPS
- $J/\psi + \psi(2S)$  signal:
  - a) 3 interfering BWs from A (fixed) + stand-alone 4<sup>th</sup> resonance
  - $\beta$ ) single resonance





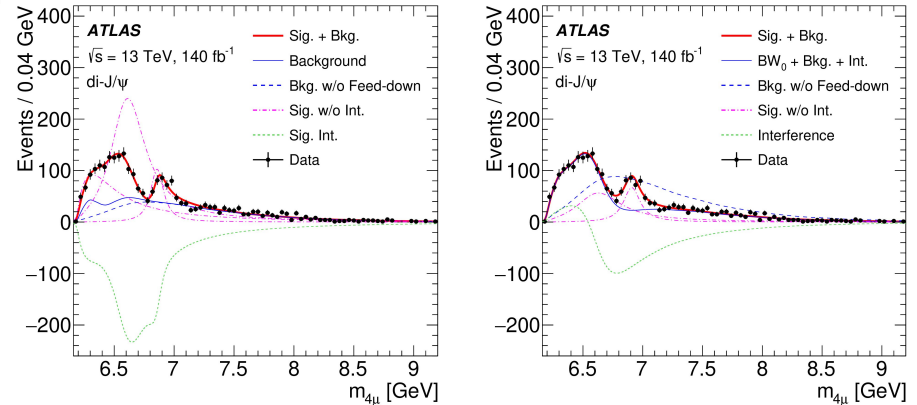
# X(6900) at ATLAS

**di-J/ψ:** models A and B describe the spectrum better than models with fewer/no interference.

**Significance for all resonances and for X(6900) alone greater than 5σ**

The broad structure at low mass could result from other physical effects (e.g. feed-down from higher di-charmonium resonances)

fitted mass in SR, Model A (left) and Model B (right)

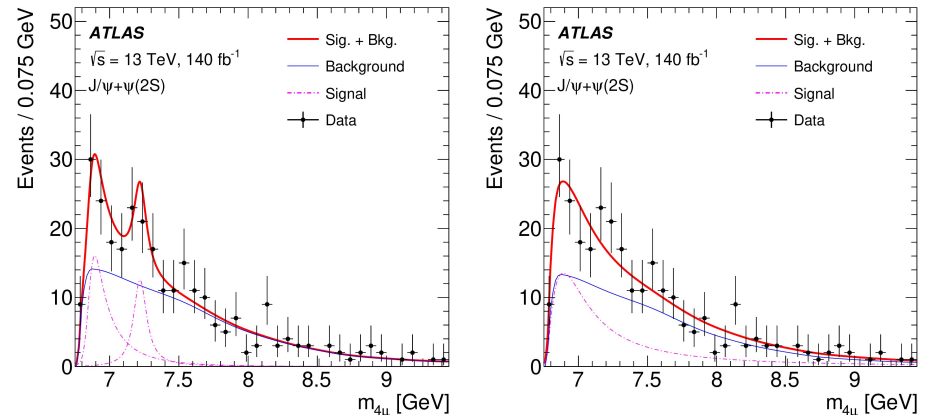


**J/ψ+ψ(2S):** significance for all resonances with model α (β) is 4.7σ (4.3σ)

Structure at 7.2 GeV alone in model α: 3.0σ

**More statistics will help to better understand the structures in both channels**

fitted mass in SR, Model α (left) and Model β (right)



# Di-charmonium production at ATLAS

Measurement of **differential production cross-sections of prompt and non-prompt  $J/\psi$  and  $\psi(2S)$**  at ATLAS using  $140 \text{ fb}^{-1}$  of pp collisions at  $\sqrt{s} = 13 \text{ TeV}$

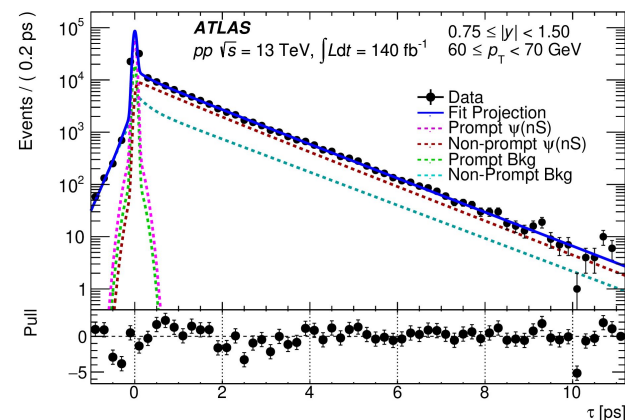
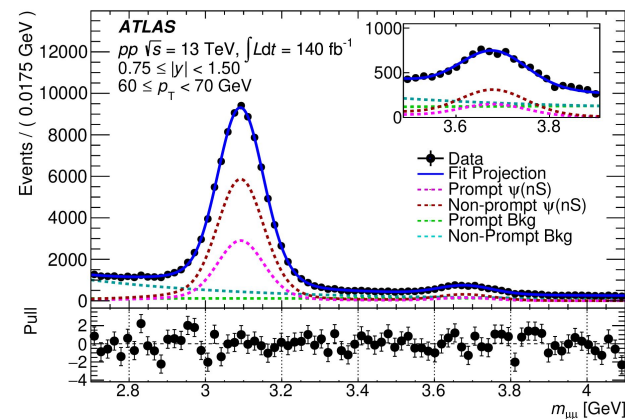
Extended probed phase-space wrt previous ATLAS measurements ( $\sqrt{s} = 7, 8 \text{ TeV}$ , [EPJ C 76 \(2016\) 283](#)) using different trigger strategies. 102 ( $p_T, y$ ) analysis bins defined in the range:

- $J/\psi$ :  $8 < p_T < 360 \text{ GeV}$ ,  $|y| < 2$
- $\psi(2S)$ :  $8 < p_T < 140 \text{ GeV}$ ,  $|y| < 2$

In each analysis bin, 2D UML fit to extract signal yield:

- di-muon invariant  $m_{\mu\mu}$
- pseudo-proper decay time  $\tau$

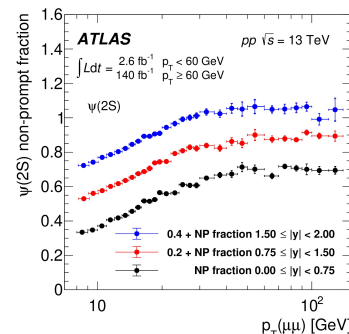
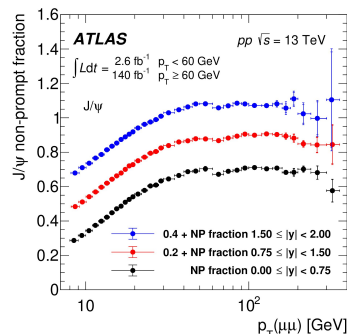
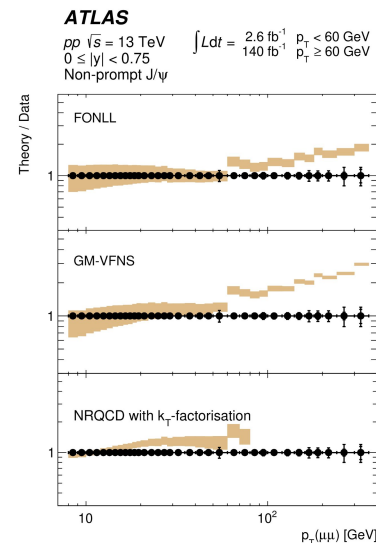
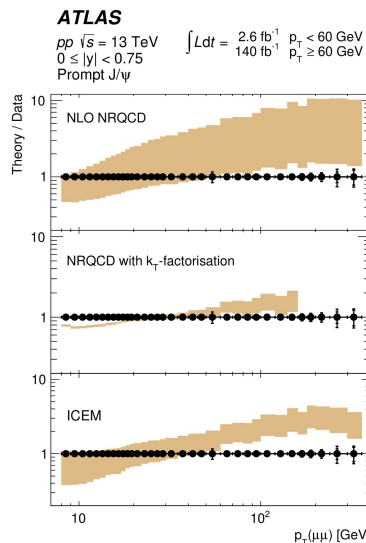
Signal yield is corrected bin-by-bin by overall efficiency (acceptance, trigger and reconstruction efficiency from MC)



# (Non-)prompt J/ψ / ψ(2S) production

- **Comparison with predictions from different theoretical models** done separately for prompt (left) and non-prompt (right) J/ψ [plots for ψ(2S) in backup]
- Predictions largely overlap considering theoretical uncertainties
- For prompt production predictions systematically have a harder spectrum, description at  $p_T > 100$  GeV needs improvement
- **Extended  $p_T$  reach can provide input to refine the theoretical models**

P and NP: similar  $p_T$ -dependence for  $p_T(\mu\mu) > 100$  GeV for both J/ψ and ψ(2S)



# Study of $\Xi_b^- \rightarrow \psi(2S)\Xi^-$ at CMS

$\Xi_b$  baryon family:  $bsq$  iso-doublets ( $\Xi_b$  (g.s.),  $\Xi_b'$ ,  $\Xi_b^*$ , according to  $j_{qs}$  and  $J^P$ )

First observation of  $\Xi_b^- \rightarrow \psi(2S)\Xi^-$  (+ c.c.) at CMS using  $140 \text{ fb}^{-1}$  of pp collisions at  $\sqrt{s} = 13 \text{ TeV}$  (2016-2018)

$$R = \frac{\mathcal{B}(\Xi_b^- \rightarrow \psi(2S)\Xi^-)}{\mathcal{B}(\Xi_b^- \rightarrow J/\psi\Xi^-)} = 0.84_{-0.19}^{+0.21}(\text{stat}) \pm 0.10(\text{syst}) \pm 0.02(\mathcal{B})$$

- $\Xi_b^- \rightarrow \psi(2S)\Xi^-$
- $\Xi_b^- \rightarrow J/\psi\Xi^-$  (norm.)
- $\Xi_b^- \rightarrow J/\psi\Lambda^0 K^-$
- $\Xi_b^- \rightarrow J/\psi\Sigma^0 K^-$

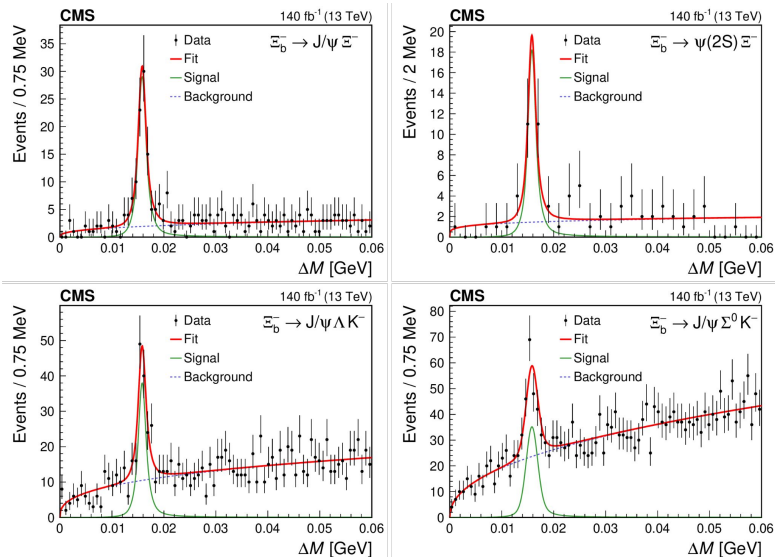
- $\psi(2S) \rightarrow \mu^+\mu^-$  or  $\mu^+\mu^-\pi^+\pi^-$
- $J/\psi \rightarrow \mu^+\mu^-$
- $\Xi^- \rightarrow \Lambda^0\pi^-; \Lambda^0 \rightarrow p\pi^-\Sigma^0 \rightarrow \Lambda^0\gamma_{\text{lost}}$

$\Xi_b^{*0}$  reconstructed in  $\Xi_b^- \pi^+$  ( $p_T > 15 \text{ GeV}$  and  $|\eta| < 2.4$ ): structure not present in same-sign  $\Xi_b^- \pi^-$  control region

Improved precision on  $\Xi_b^{*0}$  mass and width wrt previous CMS measurement ( $5 \text{ fb}^{-1}$ ) and in agreement with LHCb results [[JHEP 05 \(2016\) 161](#), [PRL 131 \(2023\) 171901](#)]

Measurement of  $\Xi_b^{*0}/\Xi_b^-$  production rate in agreement with LHCb result

$$R_{\Xi_b^{*0}} = 0.23 \pm 0.04(\text{stat}) \pm 0.02(\text{syst})$$



# $\Xi_b$ excited states at LHCb

Study of  $\Xi_b^0 \pi^+ \pi^-$  and  $\Xi_b^- \pi^+ \pi^-$  at LHCb using  $9 \text{ fb}^{-1}$  of pp collisions (7, 8, 13 TeV), together with  $\Xi_b^0 \rightarrow \Xi_c^+ \pi^- \pi^+ \pi^-$  decay observed for the first time

$\Xi_b^{(\cdot, 0)}$  combined with one charged pion or two opposite-sign pions  
Additional requirement on  $\Xi_b^{(\cdot, 0)} \pi^+ \pi^-$ : intermediate  $\Xi_b^{*0}, \Xi_b^{*-}$  or  $\Xi_b^{*-}$

- $\Xi_b^- \rightarrow \Xi_c^0 \pi^-$  or  $\Xi_c^0 \pi^- \pi^+ \pi^-$
- $\Xi_b^0 \rightarrow \Xi_c^+ \pi^-$  or  $\Xi_c^+ \pi^- \pi^+ \pi^-$
- $\Xi_c^0 \rightarrow p K^- K^+ \pi^+$
- $\Xi_c^+ \rightarrow p K^+ \pi^+$

## $\Xi_b^-(6100)$ observed at CMS now confirmed ( $12\sigma$ )

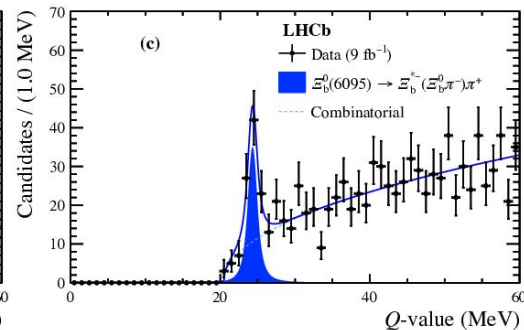
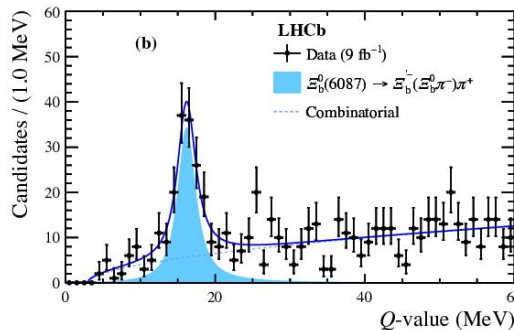
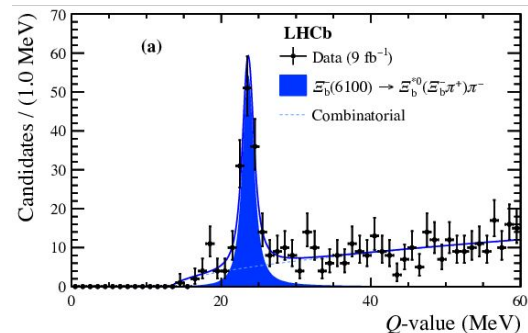
$\Gamma = (0.94 \pm 0.30 \text{ (stat.)} \pm 0.08 \text{ (syst.)}) \text{ MeV}$

CMS set CL@95%:  $\Gamma < 1.9 \text{ MeV}$  [[PRL 126 \(2021\) 252003](#)]

## First observation of two baryonic structures in $\Xi_b^0 \pi^+ \pi^-$ ( $10\sigma$ and $8\sigma$ )

Final states with up to 9 tracks: excellent momentum resolution and PID improve mass and width resolution of known baryons

Further statistics is needed to understand spin-parity and better study the spectrum



# Search for pentaquarks at LHCb

First observation of  $\Lambda_b^0 \rightarrow D^+ D^- \Lambda$  and  $\Lambda_b^0 \rightarrow D^{*+} D^- \Lambda$  (as partially reconstructed) at LHCb using  $5.3 \text{ fb}^{-1}$  of pp collisions at  $\sqrt{s} = 13 \text{ TeV}$  (2016-2018)

Reference channel:  $B^0 \rightarrow D^+ D^- K_s^0$  (known BF)

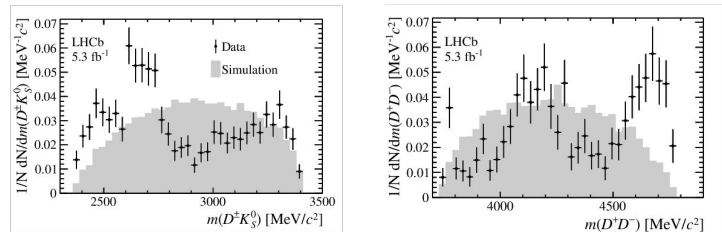
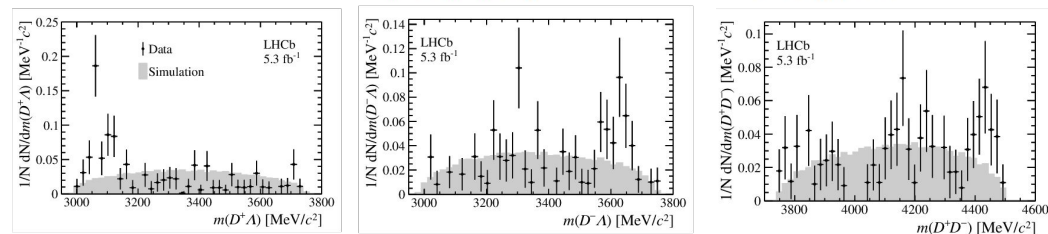
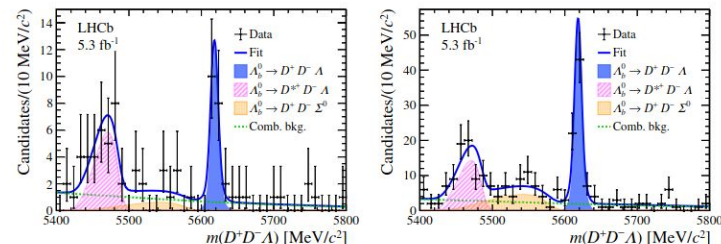
$$B(\Lambda_b^0 \rightarrow D^+ D^- \Lambda) = (1.24 \pm 0.15 \pm 0.10 \pm 0.28 \pm 0.11) \times 10^{-4},$$

$D^\pm \Lambda$  and  $D^+ D^-$  invariant mass distributions are probes for potential intermediate resonances:

- $\Xi_c^{*+} \rightarrow D^+ \Lambda$
- $D^+ D^-$  bound state (e.g.  $X(3700)$ ) can be produced near mass threshold
- open-charmed pentaquark  $P_{cs}$  can be present in the  $D^- \Lambda$  final state

Search on both signal (top) and control (bottom) channels: **deviations from phase-space suggest presence of intermediate states**

- $D^+ \rightarrow K^- \pi^+ \pi^+$
- $D^{*+} \rightarrow D^+ \pi^0$
- $K_s^0 \rightarrow \pi^+ \pi^-$
- $\Lambda \rightarrow p \pi^-$



# Prompt production of pentaquarks at LHCb

**No significant signals found** in the **search for hidden-charm** ( $\Sigma_c \underline{D}^{(*)}, \Sigma_c^* \underline{D}^{(*)}, \Lambda_c^+ \underline{D}^{(*)}, \Lambda_c^+ \pi \underline{D}^{(*)}, + \text{c.c.}$ ) and **doubly-charmed pentaquarks** ( $\Sigma_c D^{(*)}, \Sigma_c^* D^{(*)}, \Lambda_c^+ D^{(*)}, \Lambda_c^+ \pi D^{(*)}, + \text{c.c.}$ ) using  $5.7 \text{ fb}^{-1}$  of pp data at  $\sqrt{s} = 13 \text{ TeV}$

**Signal yields for known pentaquarks**  $P_c(4312)^+, P_c(4440)^+, P_c(4457)^+$  are also **consistent with zero**

Upper limit is set on 20 channels (out of 30) with enough statistics ( $>30$  candidates)

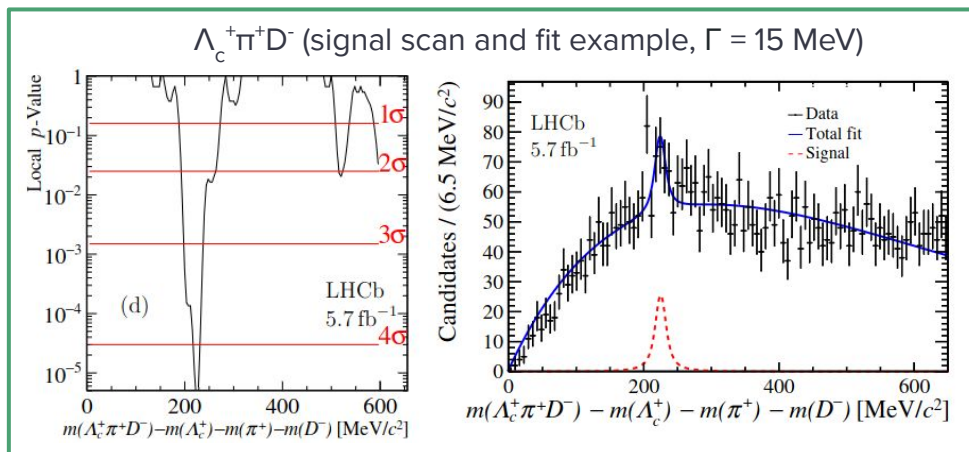
**Pentaquarks predicted to be narrow**  $\rightarrow$  Voigtian ( $\sigma_{\text{resol}} \sim 4 \text{ MeV}, \Gamma = 5, 10, 15 \text{ MeV}$ )  
sig+bkg hypothesis tested against bkg-only independently in each channel

- $\Lambda_c^+ \rightarrow p K^- \pi^+$  (norm.)
- $D^0 \rightarrow K^- \pi^+$
- $D^+ \rightarrow K^- \pi^+ \pi^+$

Pentaquark signal mass scan in steps of 4 MeV

**Excesses observed in few channels** for signals with  $\Gamma = 15 \text{ MeV}$  (largest excess in  $\Lambda_c^+ \pi^+ D^-$  of  $4.5\sigma$ ) are **compatible with statistical fluctuations**

Evaluation with 1000 MC pseudo-experiments to verify the background fluctuation



# Observation of multibody decay with $J/\psi\Xi^-$ at CMS

First observation of  $\Lambda_b^0 \rightarrow J/\psi\Xi^-K^+$  (+ c.c.) at CMS using  $140 \text{ fb}^{-1}$  of pp collisions at  $\sqrt{s} = 13 \text{ TeV}$  (2016-2018)

Normalization channel:  $\Lambda_b^0 \rightarrow \psi(2S)\Lambda$  (similar kinematics)

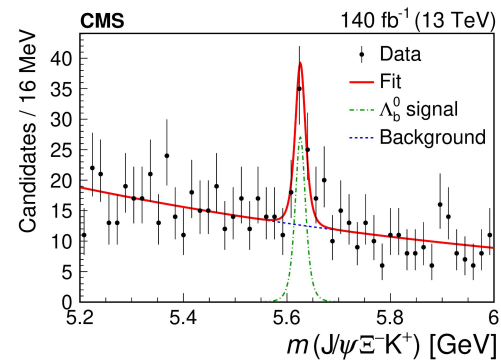
$$R = \frac{\mathcal{B}(\Lambda_b^0 \rightarrow J/\psi\Xi^-K^+)}{\mathcal{B}(\Lambda_b^0 \rightarrow \psi(2S)\Lambda)} = [3.38 \pm 1.02 \pm 0.61 \pm 0.03]\%$$

(stat)      (syst)      (BF)

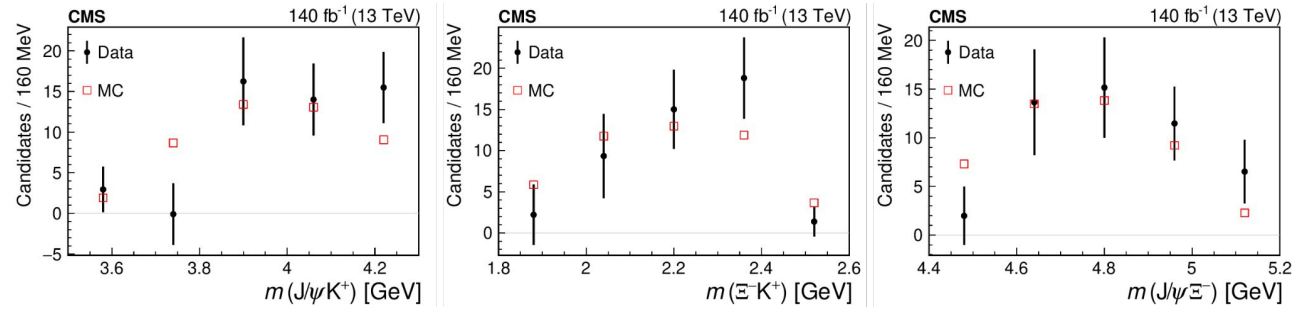
- $\psi(2S) \rightarrow \mu^+\mu^-\pi^+\pi^-$
- $J/\psi \rightarrow \mu^+\mu^-$
- $\Xi^- \rightarrow \Lambda\pi^-; \Lambda \rightarrow p\pi^-$

**Search for intermediate resonances limited by the low signal yield:**  $N(\Lambda_b^0 \rightarrow J/\psi\Xi^-K^+) = 46 \pm 11$

Bkg-subtracted distributions (sPlot) to search for intermediate resonances are shown



**First discovered multibody decay with  $J/\psi\Xi^-$ :** possible search for doubly-strange hidden-charm pentaquarks as intermediate resonance





- **LHC provides high luminosity (heavy flavor production cross section several order of magnitudes greater than at  $e^+e^-$  colliders) and the possibility to study heavy hadrons such as  $B_c$  and beauty baryons, which are not produced at Belle / Belle II.**
- **The LHC experiments are able to investigate various aspects of the heavy flavour physics and explore different phase space regions, thus complementing each other and providing valuable input for theoretical predictions**
- **As more pp collisions data are collected, new particles arise and are confirmed independently from different experiments. Many new multi-body decays are now accessible and represent a promising field to search for exotic hadrons once more statistics will be available.**

**THANKS FOR  
YOUR ATTENTION**

contacts:

[vincenzo.mastrapasqua@ba.infn.it](mailto:vincenzo.mastrapasqua@ba.infn.it)

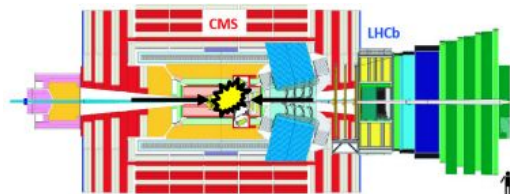
[vincenzo.mastrapasqua@cern.ch](mailto:vincenzo.mastrapasqua@cern.ch)

# X(6900) at LHCb in 2020

$J/\psi J/\psi$  ( $\rightarrow 4\mu$ ) spectrum studied at LHCb using  $9 \text{ fb}^{-1}$  of pp collisions at  $\sqrt{s} = 7, 8, 13 \text{ TeV}$

Phase-space investigated by LHCb:

- $2 < \eta < 5$
- $p_{T}(\mu) > 0.65 \text{ GeV}$
- $p(\mu) > 6 \text{ GeV}$

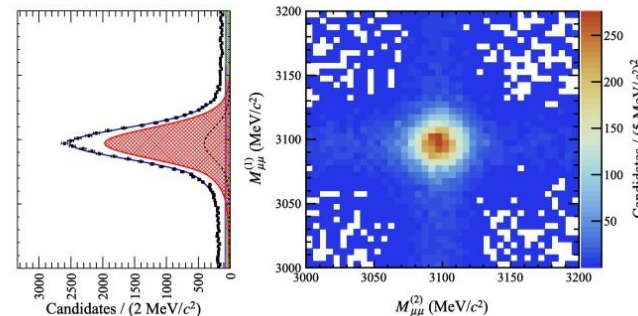
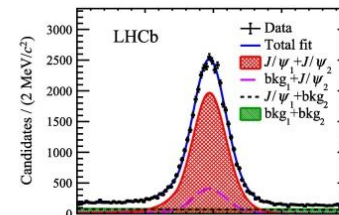


Background contribution for  $J/\psi$  pair production:

- Non-Resonant Single Parton Scattering (NRSPS)
- Non-Resonant Double Parton Scattering (DPS)

Two structures are reported:

- A broad structure near the di- $J/\psi$  mass threshold
- **A narrow resonance, X(6900), renamed  $T_{\psi\psi}(6900)$**



# The CMS detector at the Large Hadron Collider

General purpose detector with **cylindrical symmetry** and (almost) **full coverage of the solid angle**

## CMS DETECTOR

Total weight : 14,000 tonnes  
Overall diameter : 15.0 m  
Overall length : 28.7 m  
Magnetic field : 3.8 T

STEEL RETURN YOKE  
12,500 tonnes

SILICON TRACKERS

Pixel ( $100 \times 150 \mu\text{m}$ )  $\sim 1\text{m}^2$   $\sim 66\text{M}$  channels  
Microstrips ( $80 \times 180 \mu\text{m}$ )  $\sim 200\text{m}^2$   $\sim 9.6\text{M}$  channels

SUPERCONDUCTING SOLENOID

Niobium titanium coil carrying  $\sim 18,000\text{A}$

MUON CHAMBERS

Barrel: 250 Drift Tube, 480 Resistive Plate Chambers  
Endcaps: 540 Cathode Strip, 576 Resistive Plate Chambers

PRESHOWER

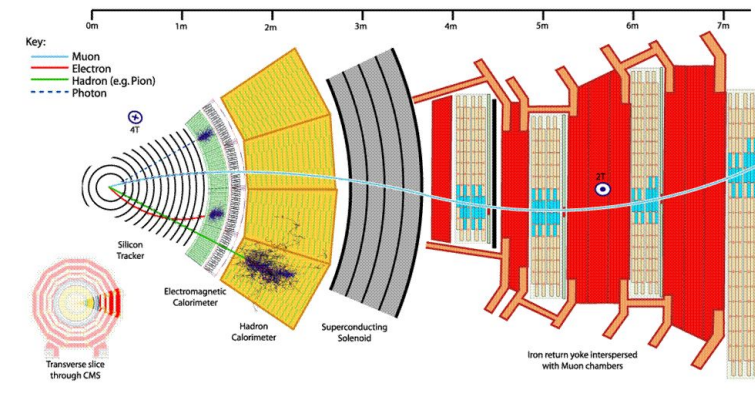
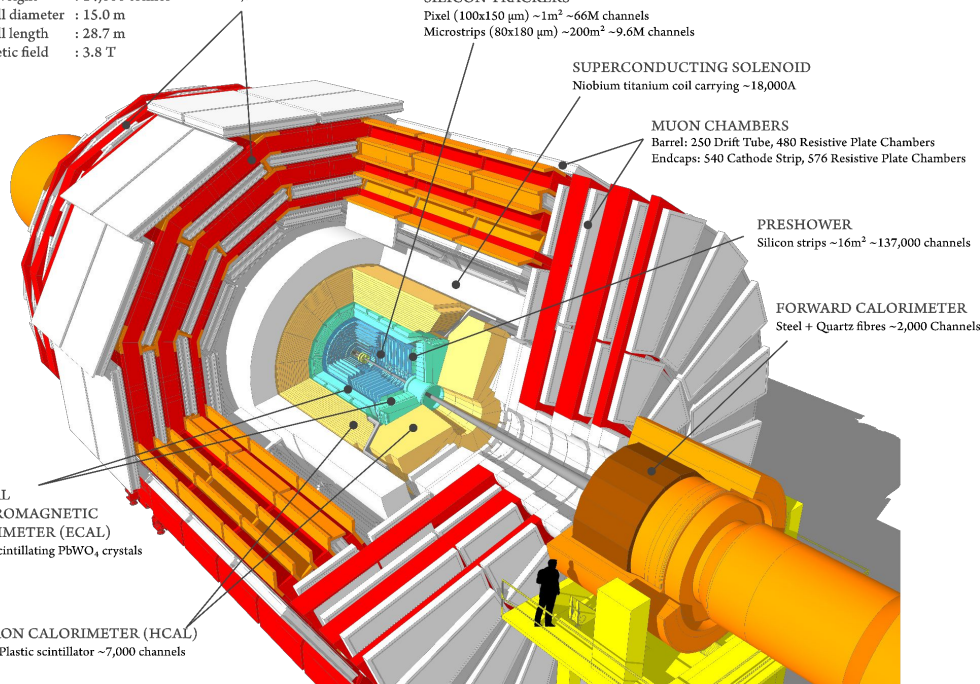
Silicon strips  $\sim 16\text{m}^2$   $\sim 137,000$  channels

FORWARD CALORIMETER

Steel + Quartz fibres  $\sim 2,000$  Channels

CRYSTAL ELECTROMAGNETIC CALORIMETER (ECAL)  
 $\sim 76,000$  scintillating  $\text{PbWO}_4$  crystals

HADRON CALORIMETER (HCAL)  
Brass + Plastic scintillator  $\sim 7,000$  channels



## Strengths:

- muon reconstruction and identification
- large muons' acceptance
- high-performance tracking & vertexing

# X(6900) at CMS: event selection

$J/\psi J/\psi$  ( $\rightarrow 4\mu$ ) spectrum studied at CMS using  $135 \text{ fb}^{-1}$  of pp collisions at  $\sqrt{s} = 13 \text{ TeV}$  (2016-2018)

## Event selection and reconstruction:

- **3- $\mu$  trigger:**  $\mu^+\mu^-$  from  $J/\psi$  + third muon (on muons from  $J/\psi$ :  $p_T(\mu^+\mu^-) > 3.5 \text{ GeV}$  in 2017-2018)
- **blinded signal region  $m(J/\psi J/\psi)$  in [6.2, 7.8] GeV** (from preliminary investigation on 2011-2012 data)
- four muons:  $p_T(\mu) > 2.0 \text{ GeV}$ ,  $|\eta(\mu)| < 2.4$ , “soft muon” identification JINST 7 (2012) P10002
- $m(\mu^+\mu^-)$  in [2.95, 3.25] GeV;  $p_T(\mu^+\mu^-) > 3.5 \text{ GeV}$   $P_{\text{vtx}}(\mu^+\mu^-) > 0.5\%$
- common vertex fit:  $P_{\text{vtx}}(4\mu) > 0.5\%$
- Arbitration of multiple candidates:
  - Select best combination of same  $4\mu$  (from MC: 0.2%)
  - Keep all candidates arising from more than four muons (from MC: 0.2%)

$$\chi_m^2 = \left( \frac{m_1(\mu^+\mu^-) - M_{J/\psi}}{\sigma_{m_1}} \right)^2 + \left( \frac{m_2(\mu^+\mu^-) - M_{J/\psi}}{\sigma_{m_2}} \right)^2$$

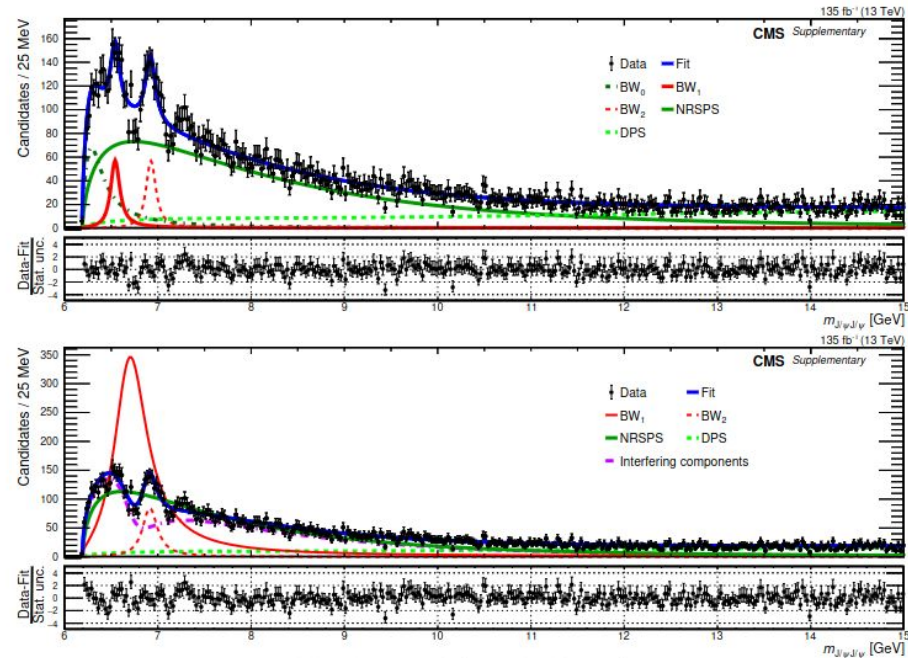
# X(6900) at CMS: fit with LHCb model

The LHCb signal models are also tested:

similar results, but worse fit quality

## LHCb signal models + CMS background

- **Model 1**  
[NRSPS+DPS+X(6900)+2BW below 6900]
  - X(6900) parameters in agreement
  - but dip at 6.7 not well described
- **Model 2:**  
[NRSPS+DPS+X(6900)+1BW below 6900 interfering with NRSPS]
  - Larger X(6700) amplitude
  - X(7300) region not well described



# X(6900) at ATLAS: event selection and results

$J/\psi J/\psi$  and  $J/\psi + \psi(2S)$  in  $4\mu$  final state studied at ATLAS using  $140 \text{ fb}^{-1}$  of  $pp$  at  $\sqrt{s} = 13 \text{ TeV}$

Prompt (SPS, DPS) and non-prompt ( $b\bar{b} \rightarrow J/\psi J/\psi + X$ ) background contributions are considered

Feed-down included only for di-Jpsi channel

## Event selection, reconstruction and definition of signal and control regions

Signal region	Control region	Nonprompt region
Dimuon or trimuon triggers, oppositely charged muons from each charmonium, loose muons, $p_{\perp}^{1,2,3,4} > 4, 4, 3, 3 \text{ GeV}$ and $ \eta_{1,2,3,4}  < 2.5$ for the four muons, $m_{J/\psi} \in [2.94, 3.25] \text{ GeV}$ , or $m_{\psi(2S)} \in [3.56, 3.80] \text{ GeV}$ , Loose vertex requirements $\chi_{4\mu}^2/N < 40$ ( $N = 5$ ) and $\chi_{\text{di-}\mu}^2/N < 100$ ( $N = 2$ ),		
Vertex $\chi_{4\mu}^2/N < 3$ , $L_{xy}^{4\mu} < 0.2 \text{ mm}$ , $ L_{xy}^{\text{di-}\mu}  < 0.3 \text{ mm}$ , $m_{4\mu} < 11 \text{ GeV}$ ,		Vertex $\chi_{4\mu}^2/N > 6$ ,
$\Delta R < 0.25$ between charmonia	$\Delta R \geq 0.25$ between charmonia	or $ L_{xy}^{\text{di-}\mu}  > 0.4 \text{ mm}$

Fit results

Di- $J/\psi$	Model A	Model B
$m_0$	$6.41 \pm 0.08_{-0.03}^{+0.08}$	$6.65 \pm 0.02_{-0.02}^{+0.03}$
$\Gamma_0$	$0.59 \pm 0.35_{-0.20}^{+0.12}$	$0.44 \pm 0.05_{-0.05}^{+0.06}$
$m_1$	$6.63 \pm 0.05_{-0.01}^{+0.08}$	...
$\Gamma_1$	$0.35 \pm 0.11_{-0.04}^{+0.11}$	...
$m_2$	$6.86 \pm 0.03_{-0.02}^{+0.01}$	$6.91 \pm 0.01 \pm 0.01$
$\Gamma_2$	$0.11 \pm 0.05_{-0.01}^{+0.02}$	$0.15 \pm 0.03 \pm 0.01$
$\Delta s/s$	$\pm 5.1\%_{-8.9\%}^{+8.1\%}$	...

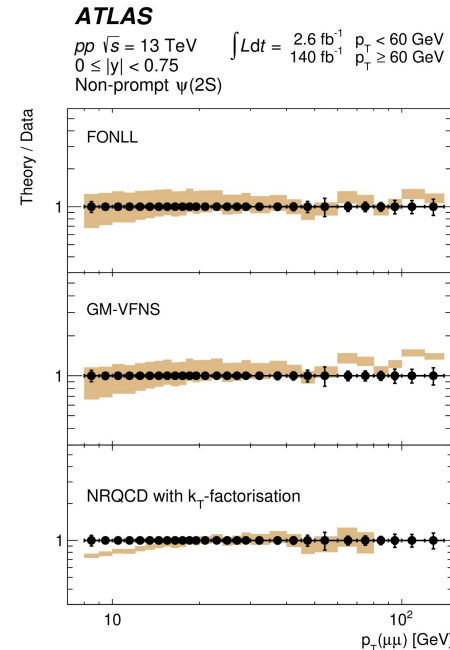
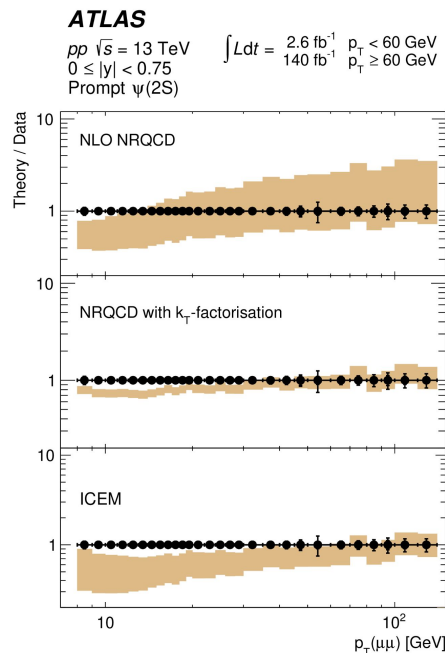
$J/\psi + \psi(2S)$	Model $\alpha$	Model $\beta$
$m_3$	$7.22 \pm 0.03_{-0.04}^{+0.01}$	$6.96 \pm 0.05 \pm 0.03$
$\Gamma_3$	$0.09 \pm 0.06_{-0.05}^{+0.06}$	$0.51 \pm 0.17_{-0.10}^{+0.11}$
$\Delta s/s$	$\pm 21\%_{-15\%}^{+25\%}$	$\pm 20\% \pm 12\%$

# (Non-)prompt $J/\psi$ / $\psi(2S)$ production

## Comparison with predictions from different theoretical models

done separately for prompt (left) and non-prompt (right) contributions

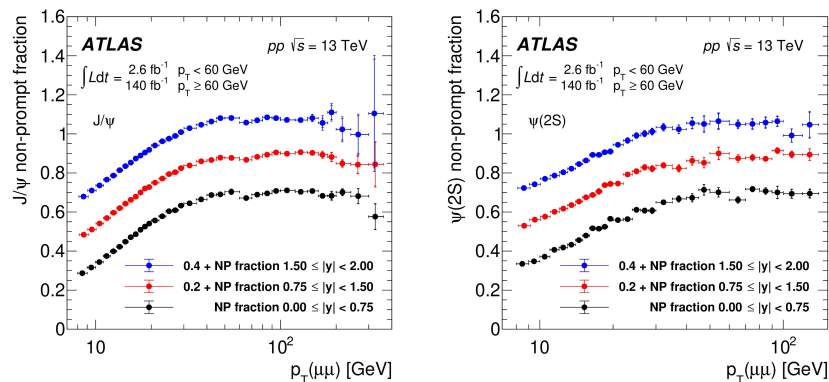
Predictions largely overlap considering theoretical uncertainties. Extended  $p_T$  reach can provide input to refine the theoretical models



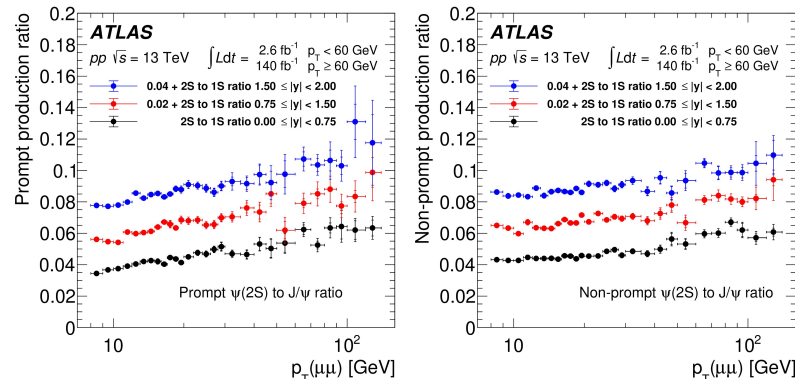


# (Non-)prompt J/ψ / ψ(2S) production

P and NP: similar  $p_T$ -dependence for  $p_T(\mu\mu) > 100$  GeV



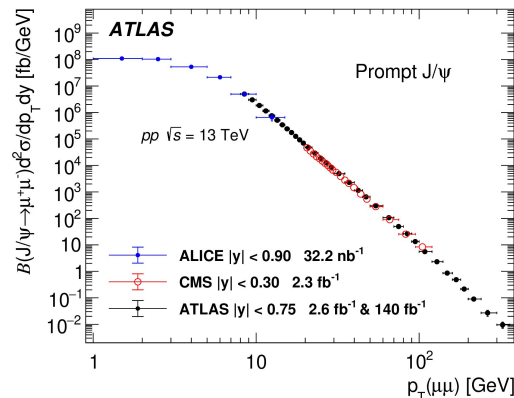
ψ(2S)-to-J/ψ production ratios



**ATLAS extended the phase-space probed by the other LHC experiments**

Differential production cross-section for prompt-J/ψ in similar rapidity range:

- CMS:
- ALICE:



# New excited beauty strange baryon into $\Xi_b^- \pi^+ \pi^-$ (CMS)

Search on  $140 \text{ fb}^{-1}$  of pp collisions data at  $\sqrt{s} = 13 \text{ TeV}$  during 2016-2018 at LHC

$\Xi_b$  baryon family: *bsq* iso-doublets (g.s.:  $\Xi_b, \Xi_b', \Xi_b^*$ , according to  $j_{qs}$  and  $J^P$ )

Search for  $\Xi_b^-$  excited states in  $\Xi_b^- \pi^+ \pi^-$ , with  $\Xi_b^-$  reconstructed in:

- |   |   |
|---|---|
| 1) $\Xi_b^- \rightarrow J/\psi \Xi^-$         | • $J/\psi^- \rightarrow \mu^+ \mu^-$                    |
| 2) $\Xi_b^- \rightarrow J/\psi \Lambda^0 K^-$ | • $\Xi^- \rightarrow \Lambda^0 \pi^-$                   |
| 3) $\Xi_b^- \rightarrow J/\psi \Sigma^0 K^-$  | • $\Lambda^0 \rightarrow p \pi^-$                       |
|   | • $\Sigma^0 \rightarrow \Lambda^0 \gamma_{\text{soft}}$ |

soft photon **not** reconstructed

## Event selection for $\Xi_b^-$ reconstruction:

- combination of **triggers targeting  $J/\psi \rightarrow \mu^+ \mu^-$**
- $p_T(\mu) > 3 \text{ GeV}$ ;  $|\ln(\mu)| < 2.4$ ;  $P_{\text{vtx}}(\mu\mu) > 1\%$ ;  $|\ln(\mu\mu) - M_{J/\psi}^{\text{PDG}}| < 100 \text{ MeV}$
- $|\ln(p\pi^-) - M_{\Lambda}^{\text{PDG}}| < 10 \text{ MeV}$ ;  $p_T(\Lambda) > 1 \text{ GeV}$ ;  $P_{\text{vtx}}(p\pi^-) > 1\%$
- **Further selection separately optimized for each decay channel**, including selection on  $\Xi_b^-$  flight distance and its alignment with  $\Xi_b^-$  momentum

# $\Xi_b^-$ signal extraction: UML fit to data (CMS)

- **Fully reconstructed signals:**  
Double-Gaussian (resolution from MC)
- **Partially reconstructed signal:**  
Asymmetric Gaussian (shape from MC)
- **Combinatorial background:**
  - $J/\psi\Xi^-$ : 1<sup>st</sup> order polynomial
  - $J/\psi\Lambda K^-$ : exponential function

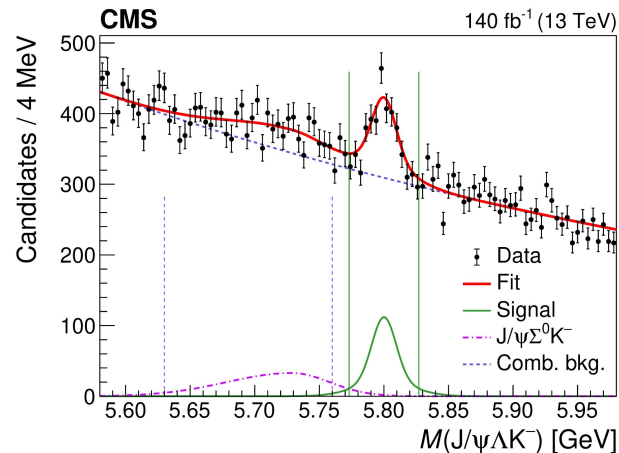
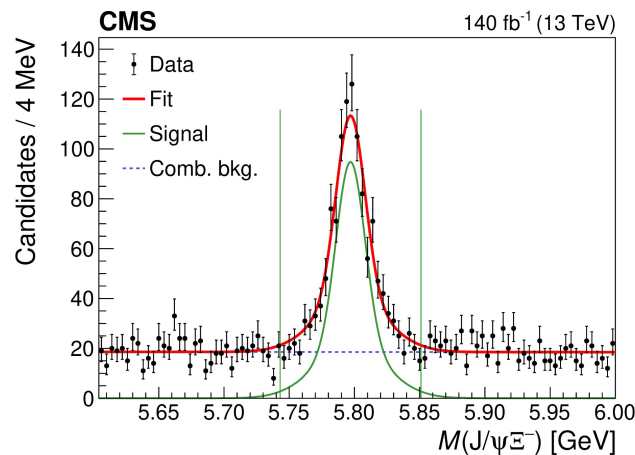
$N(\Xi_b^- \rightarrow J/\psi\Xi^-) = 859 \pm 36$  events

$N(\Xi_b^- \rightarrow J/\psi\Lambda^0 K^-) = 815 \pm 74$  events

$N(\Xi_b^- \rightarrow J/\psi\Sigma^0 K^-) = 820 \pm 158$  events

## Excited $\Xi_b^-$ candidates' reconstruction:

- Mass windows for  $\Xi_b^-$  candidates (see plots)
- Two OS tracks from same PV as  $\Xi_b^-$   
(negligible  $\tau(\Xi_b^-) \simeq 1.6$  ps)
- Control region: SS tracks from same PV as  $\Xi_b^-$
- Mass variable  $\Delta M = m(\Xi_b^- \pi^+ \pi^-) - m(\Xi_b^-) - 2m_{\pi}^{PDG}$   
(insensitive to potential mass shift due to lost  $\gamma_{\text{soft}}$ )



# Excited $\Xi_b^-$ signal extraction (CMS)

**Dominant contribution of intermediate  $\Xi_b^{*0}$ :**  $\Xi_b^{*-} \rightarrow \Xi_b^{*0} \pi^-$ ,  $\Xi_b^{*0} \rightarrow \Xi_b^- \pi^+$  is suggested by analogy with  $\Xi_c$  family and theoretical studies

**Additional cut:**  $m(\Xi_b^{*0}) - m(\Xi_b^-) + m_\pi^{\text{PDG}} < 20.73 \text{ MeV}$   
(peak expected at 15.73 MeV)

**Fully reconstructed channels are combined**  
(same resolution,  $\Xi_b^- \rightarrow J/\psi \Sigma^0 K^-$  30% larger res.)

**UML simultaneous fit:**

- **Signal:** Relativistic BW $\otimes$ Double-Gaussian
- **Background:**  $(\Delta M)^\alpha$  threshold function

$M(\Xi_b^{*-}) = 6100.3 \pm 0.2(\text{stat}) \pm 0.1(\text{syst}) \pm 0.6(\Xi_b^-) \text{ MeV}$   
 $\Gamma(\Xi_b^{*-}) < 1.9 \text{ MeV @ CL=95\%}$   
 (narrow resonance, 13 MeV below  $\Lambda_b^0 K^-$  threshold)  
 Local statistical significance: 6.2-6.7 $\sigma$

**The decay sequence suggest:**  $j_{\text{QS}} = 1$ ,  $J^P = 3/2^-$   
**beauty partner of the charmed  $\Xi_c(2815)$  baryon**

